HHS Public Access

Author manuscript

J Surg Res. Author manuscript; available in PMC 2020 June 01.

Published in final edited form as:

J Surg Res. 2019 June ; 238: 152–163. doi:10.1016/j.jss.2019.01.028.

Intrahepatic delivery of pegylated-catalase is protective in a rat ischemia/reperfusion injury model

Clifford Akateh[1,2,3], **Eliza W. Beal**[1,2,3], **Jung-Lye Kim**[1], **Brenda F. Reader**[1,2,3], **Katelyn Maynard**[1], **Jay L. Zweier**[4], **Bryan A. Whitson, MD, PhD**[1,2,3], **Sylvester M. Black, MD, PhD**[1,2,3]

[1]The COPPER Laboratory, The Ohio State University Wexner Medical Center, Columbus, OH 43210

[2]Comprehensive Transplant Center, The Ohio State University Wexner Medical Center, Columbus, OH 43210

[3]Department of Surgery, The Ohio State University Wexner Medical Center, Columbus, OH 43210

[4]Department of Internal Medicine, The Ohio State University Wexner Medical Center, Columbus, OH 43210

Abstract

Background: Ischemia/reperfusion injury (IRI) can occur during liver surgery. Endogenous catalase is important to cellular antioxidant defenses and is critical to IRI prevention. Pegylation of catalase (PEG-CAT) improves its therapeutic potential by extending plasma half-life, but systemic administration of exogenous PEG-CAT has been only mildly therapeutic for hepatic IRI. Here, we investigated the protective effects of direct intrahepatic delivery of PEG-CAT during IRI using a rat hilar clamp model.

Materials and Methods: PEG-CAT was tested in vitro and in vivo. In vitro, enriched rat liver cell populations were subjected to oxidative stress injury (H_2O_2), and measures of cell health and viability were assessed. In vivo, rats underwent segmental (70%) hepatic warm ischemia for 1 hour, followed by 6 hours of reperfusion, and plasma ALT and AST, tissue MDA, ATP, and GSH, and histology were assessed.

Corresponding Author: Sylvester M. Black, MD, PhD, Assistant Professor of Surgery, The Ohio State University, Wexner Medical Center, 395 W. 12th Ave, Suite 150, Columbus, OH 43210, Phone: (614) 293-3212, Fax: (614) 293-6720, Sylvester.Black@osumc.edu.

Author Contributions

SMB conceived of the study objectives and design. CA, EWB, JLK, KM collected and analyzed data. CA, EWB, JLK, BFR, KM, JLZ, BAW, and SMB interpreted the findings. CA and EWB drafted the manuscript. CA, EWB, JLK, BFR, KM, JLZ, BAW, and SMB provided critical revision and review of the manuscript for important intellectual content and approval of the final draft to be submitted. SMB and BAW acquired funding for the study.

Disclosure

The authors declare no conflict of interest.

Results: In vitro, PEG-CAT pre-treatment of liver cells showed substantial uptake and protection against oxidative stress injury. In vivo, direct intrahepatic, but not systemic, delivery of PEG-CAT during IRI significantly reduced ALT and AST in a time-dependent manner ($P<0.01$, $P<0.0001$, respectively for all time points) compared to control. Similarly, tissue MDA ($P=0.0048$), ATP ($P=0.019$), and GSH ($P=0.0015$), and the degree of centrilobular necrosis were improved by intrahepatic compared to systemic PEG-CAT delivery.

Conclusion: Direct intrahepatic administration of PEG-CAT achieved significant protection against IRI by reducing the volume distribution and taking advantage of the substantial hepatic first-pass uptake of this molecule. The mode of delivery was an important factor for protection against hepatic IRI by PEG-CAT.

Keywords

Ischemia/Reperfusion injury; PEGylated catalase; PEG-CAT; Liver Transplantation; Hydrogen Peroxide; Hepatectomy; Oxidative Stress

Introduction

Surgical interventions on the liver require a careful balance between prevention of excessive intraoperative bleeding and the avoidance of further injury to the liver. During major hepatic resections and management of severe traumatic injuries, the portal triad (hilum) is clamped for variable durations to avoid excessive bleeding (1, 2). Prolonged clamping is limited by ischemia/reperfusion injury (IRI) to the remaining liver (3, 4), and, when there is underlying liver disease, IRI can result in postoperative liver failure (5, 6). Additionally, many primary liver cancers, such as hepatocellular carcinoma, often arise on a background of cirrhosis, increasing the risk of postoperative liver failure from IRI when resected (7). A similar concern arises during liver transplantation where the liver invariably undergoes some amount of IRI. This can be detrimental to the organ resulting in a higher risk of delayed graft function or primary non-function with early graft loss (8). As such, there is a critical need to develop effective therapeutic interventions to prevent and/or attenuate hepatic IRI.

In IRI, the restoration of blood flow after a period of ischemia causes the release of toxic metabolites and reactive oxygen species (ROS) (9). If not resolved by endogenous protective mechanisms, the resultant oxidative stress causes both direct and indirect injury to surrounding cells and tissues. This manifests as endothelial swelling, vasoconstriction, leukocyte migration and entrapment, and platelet aggregation within the sinusoids (10-13). These events lead to microvascular thromboses, failure of microcirculation, and subsequent severe organ damage. In healthy cells, oxidative stress is managed by a cellular antioxidant defense system that includes enzymes like superoxide dismutase (SOD) and catalase. SOD catalyzes the conversion of superoxide anions into hydrogen peroxide (H_2O_2) and oxygen (O_2), while catalase catalyzes the conversion of H_2O_2 to water (H_2O) and O_2 (14), thus functioning to prevent cellular damage. During severe IRI, this system becomes overwhelmed, and thus, cells are unable to meet the demand for the endogenous enzymes required for full protection (15). Finding a way to utilize exogenous antioxidants to mitigate IRI during major surgical procedures would be of great therapeutic benefit (16-18).

Pegylated-catalase (PEG-CAT) may hold great potential for clinical use in preventing hepatic IRI, but the ability of PEG-CAT to significantly protect the liver from IRI has not yet been demonstrated. An additional limitation of exogenous catalase is its short half-life, which is only a few minutes. Chemical modification of catalase by pegylation significantly increases the half-life of the enzyme to several hours while retaining about 90% of its enzymatic activity (17, 19, 20). However, when administered systemically, PEG-CAT has limited hepatic protection at reasonable doses, because it remains in the plasma and/or is taken up by other organs and tissues.

In this study, we sought to investigate the outcome of targeted intrahepatic delivery of PEG-CAT using a rat IRI hilar clamp model with portal cannulation (21). We hypothesized that a more targeted approach would improve hepatic distribution and attenuate hepatic IRI.

Materials and Methods

Animals

All in vitro and in vivo experiments used male Sprague-Dawley rats (Envigo®, Indianapolis, IN) weighing 225–250 grams. Animals were housed under standard conditions (humidity: 45% - 70%, temperature: 21 ± 3 °C, 12-hour light/dark cycle) and were provided with ad libitum access to water and standard chow diet. Animal experiments were humanely performed with approval obtained from the Ohio State University Institutional Animal Care and Use Committee (IACUC protocol # 2012A00000126-R1). All experiments were in strict accordance with the National Institutes of Health Guide for the Care and Use of Laboratory Animals (NIH Publications No. 8023, revised 1978).

Isolation and Culture of Primary Cells

Primary rat liver cells were enriched and cultured using previously described methods (22-24). Briefly, following laparotomy and exposure of abdominal contents, the liver was collagenase digested by in situ by cannulation of the inferior vena cava. For isolation of hepatocytes, Kupffer cells (KCs), and liver sinusoidal endothelial cell (LSECs), the liver was perfused sequentially with Hank’s balanced salt solution (HBSS) without calcium and with EDTA followed by 0.05% collagenase type IV in DMEM solution. Undigested liver tissue was cut into small pieces, filtered through two nylon meshes, and centrifuged at 50Xg. LSEC and KC isolation was performed with the supernatant via Percoll density gradient centrifugation. LSECs yielded ~10-15 million cells per rat with >90% viability and >92% purity as measured by flow cytometry (data not shown). KCs yielded ~5-10 million cells per rat with a >93% purity and >95% viability as measured by flow cytometry (data not shown). Hepatocytes were isolated by resuspending the pellet yielding ~100-150 million cells per rat with a >90% viability and >95% purity as measured by flow cytometry (data not shown). For hepatic stellate cell (HSC) isolation, perfusion of the rat liver differed from the above with smaller volumes of perfusate and a slower speed. Following the removal of the liver, the tissue was cut into small pieces and agitated in DMEM containing 0.5mg/ml pronase and 4-5U DNase at 37°C for 10 minutes. After centrifugation, the cell suspension was filtered through a metal sieve, and HSCs were isolated by iodixanol (15%-11%) density gradient centrifugation yielding ~10-20 million cells per rat with >95% viability and >96% purity as

measured by flow cytometry (data not shown). In vitro studies were performed in triplicate with 3-4 biological replicates per condition.

PEG-CAT (Pegylated-Catalase)

Lyophilized PEG-CAT (~40,000 units/mg protein) was obtained from a commercial source (Sigma-Aldrich; St. Louis, MO; catalog # C4963). Fresh solutions of PEG-CAT were prepared for each experiment. PEG-CAT was first dissolved in sterile water, and then diluted to the proper concentration in media.

Microscopy of Fluorescein Isothiocyanate (FITC)-Labeled PEG-CAT

The endothelium has been thought to be a preferential target for PEG-CAT during systemic delivery. We tested whether PEG-CAT was taken up by other liver cells as well. Therefore, rat hepatocytes, KCs, LSECs, or HSCs were cultured in 96 well plates (20,000 cells per well) for 24 hours at 37°C in a humidified atmosphere of 5% CO_2/95% air. Cells were then incubated for 3 hours with 625U/mL of commercially obtained PEG-CAT labeled with fluorescein isothiocyanate (FITC) (Nanocs, New York, NY). In a separate experiment,hepatocytes were cultured with 625 U/mL of FITC-labeled catalase (Nanocs, New York, NY) or FITC-labeled PEG-CAT for up to 3 hours and uptake was examined. To note, hepatocytes were used for this experiment since they compose a majority of the liver cell population and, in the literature and in our experiments, they showed the most preferential uptake of catalase(25). Images were obtained by fluorescence microscopy at 0, 1, 2, and 3 hours of incubation using the Lionheart™ FX Automated Microscope (BioTek Instruments, Winooski, Vermont). Fluorescence values were taken from 4 random fields and were normalized to cell number (1000 cells/field) for each sample using the Gen5 Microplate Reader and Imaging Software (BioTek Instruments, Winooski, VT). The amount of PEG-CAT taken up by various cell types was computed as mean fluorescence intensity where the mean fluorescence in the 0 hour time point was used to subtract background from the fluorescence values at each time point. The mean and standard deviation of these absolute differences between the time point of interest and the zero time point was graphed for each time point.

Measurement of Cell Viability

The response to oxidative stress injury during hepatic IRI is mediated largely by hepatocyte and LSECs. Therefore, hepatocytes and LSECs were cultured in 1% FBS MEM media containing varying amounts of PEG-CAT (0, 156.3, 312.5, 625, 1250 U/mL) at 37°C in a humidified atmosphere of 5% CO_2 /95% for 3 hours. Cells were then washed several times and treated with 400 μM H_2O_2 (Sigma-Aldrich Chemicals, St. Louis, MO) for 3 hours to induce oxidative stress injury. In a separate experiment, hepatocytes were cultured in 1% FBS MEM media containing 1250 U/mL of catalase (Sigma-Aldrich). Cells were then washed several times and oxidatively stressed as stated above. Cell proliferation was determined using a colorimetric assay based on the uptake of 3-(4,5-dimethylthiazol-2-yl)-2,5-diphenyl-2H-tetrazolium bromide (MTT) (DUCHEFA Biochemie, Haarlem, Netherlands) by viable cells. The cells were treated with 1 mg/mL MTT solution and incubated at 37°C in a humidified atmosphere of 5% CO_2 /95% for 3 hours resulting in the formation of blue formazan. The absorbance of formazan was measured at λ = 570 nm with

background subtraction of λ = 690 nm (Polarstar Omega, BMG LABTECH, Ortenberg, Germany).

Measurement of Mitochondrial Membrane Potential (MMP)

Hepatocyte and LSECs were cultured in 1% FBS MEM containing varying amounts of PEG-CAT (0, 156.3, 312.5, 625, 1250 U/mL) at 37°C in a humidified atmosphere of 5% CO_2 /95% in air for 3 hours. Cells were then washed several times and treated with 400 μM H_2O_2 for 3 hours. Mitochondrial membrane potential (ΔΨm) of the cells was determined by using the fluorescent JC-1 Mitochondrial Membrane Potential Assay Kit (Cayman Chemical, Ann Arbor, MI) according to the manufacturer's instructions. JC-1 is a lipophilic, cationic dye that selectively enters mitochondria and reversibly changes color from green to red as the membrane potential increases. In healthy cells with high ΔΨM, JC-1 spontaneously forms J-aggregate complex that fluoresce red. In apoptotic or unhealthy cells with low ΔΨM, JC-1 remains a monomer and fluoresces green. The green fluorescence intensities from the JC-1 monomer (λ = 530 nm excitation) and the red fluorescence intensities from the aggregated form of JC-1 (λ = 590 nm emission) in the cells were measured using the POLARstar Omega microplate reader (BMG Labtech, Ortenberg, Germany) and viewed under a microscope (Lionheart™ FX Automated Microscope, BioTek Instruments, Winooski, VT). The ratio of fluorescent intensities of the J-aggregates (red) to monomers (green) yields an indication of cell health.

Hilar Clamp Model and Intrahepatic Delivery

Ischemia was induced in rats using a hilar clamp model as previously described (21). This method allows for significant IRI to occur in the liver, while reducing the risk of mortality during the procedure. Briefly, anesthesia was induced and maintained with a continuous isoflurane anesthesia delivery system (Somnosuite/Physiosuite, Kent Scientific Corp, Torrington, CT). A midline laparotomy incision was made and extended laterally. The portal vein was identified and dissected into the liver hilum to identify portal vein branches. For intrahepatic delivery, the left portal vein was cannulated with a 27-gauge micro-cannula (Braintree Scientific, Braintree, MA). For control animals (n=6), 2 ml of DMEM (Corning, Manassas, VA) was slowly injected into the left portal vein. For treatment animals (n=6), 2 mg of 40,000 U/mg PEG-CAT was suspended in 3 ml of DMEM, and 2 ml of the suspension was slowly injected into the left portal vein. A vascular clamp was placed across the hilum of the left and median lobes of the liver, inducing ischemia to ~70% of the liver (21). After 1 hour post-initiation of ischemia, the clamp was removed, and livers were reperfused for 6 hours. Blood samples were taken prior to the induction of ischemia and at 0.5, 3, and 6 hours post-reperfusion. After 6 hours of reperfusion, the left and median lobes were procured, and the samples were snap frozen or preserved in 10% neutral buffered formalin for tissue analysis. The right and caudate lobes of the liver were not used for analysis as these did not experience IRI.

Systemic Delivery of PEG-CAT

Anesthesia was induced in rats (n=6 per group) using an isoflurane chamber and maintained with continuous isoflurane delivery. For systemic delivery, following laparotomy, the portal vein was identified and dissected into the liver hilum to identify portal vein branches. The

portal system was not cannulated, and, instead, the left femoral vein was identified and cannulated with the micro-cannula. For control animals, 2 ml of DMEM (Corning, Manassas, VA) was injected into the left femoral vein. For treatment animals, 2 mg of 40,000 U/mg PEG-CAT suspended in 3 ml of DMEM, and 2 ml was injected into the left femoral vein. Vehicle and PEG-CAT were allowed to circulate for 5 minutes to ensure that the liver was fully perfused. A vascular clamp was then placed across the hilum of the left and median lobes of the liver creating complete ischemia to these lobes (~70% liver). At 1 hour post-initiation of the ischemia, the clamp was removed, and livers were reperfused for 6 hours. Blood samples were taken prior to the start of ischemia and at 0.5, 3, and 6 hours post-reperfusion. After 6 hours of reperfusion, the left and median lobes were procured, and the samples were snap frozen or preserved in 10% neutral buffered formalin for tissue analysis.

Biochemical Analysis

Alanine aminotransferase (ALT) and aspartate aminotransferase (AST) levels were determined in sera colorimetrically using an ALT Activity Colorimetric Assay Kit and an AST Activity Colorimetric Assay Kit (Biovision, Milpitas, CA) according to manufacturer's instructions. Lipid peroxidation was quantified in liver tissue using a colorimetric Malondialdehyde (MDA) Assay kit (Abcam, Cambridge, UK) according to the manufacturer's instructions. Adenosine triphosphate (ATP) production was measured in liver tissue using the ENLITEN® ATP Assay System (Promega, Madison, WI) according to the manufacturer's instructions. Cellular total glutathione (GSH) was measured in liver tissue using the GSH/GSSG-GloTM assay kit (Promega, Madison, WI) according to manufacturer's instructions. Assays were measured using the POLARstar Omega microplate reader (BMG Labtech, Ortenberg, Germany).

Histologic Evaluation

Specimens for histology were stored in 10% neutral buffered formalin, transferred to 70% ethanol, and then paraffin embedded. Using standard methods, 5-μm sections were cut, and hematoxylin and eosin staining were performed. Tissue sections were assessed by a trained, blinded pathologist and scored using the Suzuki scoring system Suzuki (26). Sections received a score of 0-4 for sinusoidal congestion, hepatocyte vacuolization and tissue necrosis and the total score for the slide were computed.

Systemic or Intrahepatic Administration of Alexa Fluor 488-labeled PEG-CAT

We discovered during our pilot in vivo experiments that FITC-labeled PEG-CAT was subject to significant photobleaching, thus limiting the imaging and visualization of our liver sections. This photobleaching limitation was not observed with the in vitro experiments since the cells were only imaged for a short period of time. Because FITC is quite a photolabile fluorescent dye, photobleaching can occur within minutes (27). This problem was overcome by using a commercially obtained Alexa Fluor 488-labeled PEG-CAT (Nanocs, New York, NY). Alexa Fluor dyes are remarkably photostable (28) and, as such, allowed us to circumvent the issue of photobleaching for these in vivo experiments.

For intrahepatic administration, the left portal vein was cannulated as described above for the hilar clamp technique without the 1 hour of ischemia time, and Alexa Fluor 488-labeled PEG-CAT was injected as described above. For systemic administration, the femoral vein was accessed and injected with Alexa Fluor 488-labeled PEG-CAT. After administration, livers were flushed, immediately procured, and then prepared for frozen sections. The liver tissue sections were viewed with fluorescence microscopy (Lionheart™ FX Automated Microscope, BioTek Instruments, Winooski, VT).

Statistical Analyses

The results are expressed as mean ± standard deviation for each group. Significant differences between and within groups were determined by ANOVA, and were followed by Tukey's multiple comparisons test. The Student's *t*-test was used to analyze differences between 2 groups. P-values less than 0.05 were considered to be statistically significant. Analyses were performed using GraphPad Prism 7® software (LaJolla, CA). Power analyses were performed in Stata/IC 15.1 (College Station, TX: StataCorp LP).

Results

FITC-labeled PEG-CAT is Taken Up by Both Parenchymal and Non-Parenchymal Liver Cells

In vitro, we assessed the uptake of FITC-labeled PEG-CAT by primary hepatocytes, LSECs, KCs, and HSCs isolated from rat livers. Images were obtained by fluorescence microscopy at various time points (Figure 1A). Uptake of PEG-CAT was observed in all 4 cell types by the 3 hour time point. The fastest uptake occurred in hepatocytes (Figure 1B 1 hour P=0.016; 2 hours P<0.0001, 3 hours P<0.0001) and KCs (Figure 1B; 2 hours P=0.0012, 3 hours P<0.0001). While LSECs (Figure 1B; 3 hours P=0.0023) and HSCs Figure 1B; 3 hours P<0.0001) were slower to uptake PEG-CAT.

PEG-CAT Treatment Protects Hepatocytes and LSECs Exposed to H_2O_2-induced Oxidative Stress

The protective effects of PEG-CAT on primary hepatocytes and LSECs were determined by pretreating cells with varying amounts of PEG-CAT, and then subjecting the cells to H_2O_2-induced oxidative stress injury (29) (Figure 2 A-C and 3A-C). Cellular viability was measured using an MTT assay. Data indicate that pre-treatment with PEG-CAT had a dose-dependent improvement in cell viability for hepatocytes (Figure 2A; 625μM P=0.0041; 1250μM P=0.0002) and LSECs (Figure 2A; 625μM P=0.0033; 1250μM P=0.0017) in comparison to cells treated with H_2O_2 alone.

PEG-CAT Prevents Loss of Mitochondrial Membrane Potential in Hepatocytes and LSECs Exposed to Oxidative Stress

To investigate the mechanism of protection afforded by treatment with PEG-CAT, the mitochondrial membrane potential of oxidatively stressed hepatocytes and LSECs were studied using the dye JC-1 (Figure 2 B, C and Figure 3 B, C). JC-1 shows membrane potential-dependent aggregation in the mitochondria as demonstrated by a shift from red to green fluorescence. Red fluorescence indicates normal mitochondrial membrane potential or health, green fluorescence indicates depolarized mitochondrial membrane potential or

damaged mitochondria, and the red to green fluorescence ratio indicates cellular health. Hepatocytes and LSECs treated with PEG-CAT demonstrated significant maintenance of mitochondrial membrane potential compared to hepatocytes and LSECS treated with H_2O_2 alone (Figure 2B hepatocytes: 1250μM P=0.0081; Figure 3B LSECs: 156.3μM P=0.016; 312.5μM P=0.0059; 625μM P=0.0024; 1250μM P=0.0007).

Direct Intrahepatic Infusion of PEG-CAT Attenuates Serum Markers of Hepatocellular Injury

Serum levels of ALT and AST are well-accepted markers of hepatocellular injury and are used in clinical medicine to quantify the extent of liver damage/injury. To evaluate the protective effects of PEG-CAT on the liver after IRI, AST and ALT levels were analyzed in serum samples at several time points before and during IRI. Clamping of the median and left liver lobes resulted in significant elevations in AST and ALT. PEG-CAT pretreatment provided a significant reduction in these markers. Compared to base perfusate alone, ALT levels were lower at 0.5, 3, and 6 hours of reperfusion with PEG-CAT treatment (Figure 4A; 0.5 hours P=0.0021; 3 hours P<0.0001; 6 hours P<0.0001). Similarly, AST levels were lower at 0.5, 3, and 6 hours of reperfusion with PEG-CAT treatment compared to base perfusate alone (Figure 4B; 0.5 hours P<0.0001; 3 hours P<0.0001; 6 hours P<0.0001). In contrast, PEG-CAT delivered systemically by injection into the femoral vein, did not result in significantly reduced AST and ALT levels compared to base perfusate alone (Figure 4C and Figure 4D).

Several biochemical indicators of liver injury were then examined in the liver tissue collected at the termination of the experiment, i.e., 6 hours post-reperfusion. Tissue malondialdehyde (MDA) is a marker of lipid peroxidation that increases with cell damage, and the amount of lipid peroxidation, and thus cell damage, was quantified as the intensity of the pink MDA-thiobarbituric acid (TBA) conjugate present in the liver tissue. After IRI, a significant amount of lipid peroxidation was seen in the control livers, but livers that received PEG-CAT via direct intrahepatic administration showed a significant reduction in lipid peroxidation (Figure 5A; P=0.0048). In contrast, systemic administration of PEG-CAT via the femoral vein did not protect against lipid peroxidation, as MDA levels in liver tissue were not significantly different from the control IRI group (Figure 5D).

ATP stores in liver tissue were measured as a marker of mitochondrial and liver health. While IRI resulted in a significant decrease in the ATP stores in the liver tissue, data indicate that ATP production remained significantly higher in the livers administered PEG-CAT via intrahepatic delivery compared to vehicle-treated livers (Figure 5B; P=0.019). When PEG-CAT was administered systemically, there was no difference in ATP production compared to vehicle-treated livers (Figure 5E).

Given its critical role in the cellular response to stress, tissue levels of reduced glutathione (GSH) were investigated. Data indicate that vehicle-treated livers had significantly lower levels of reduced GSH following IRI, which reflect a poor response to cellular stress and reperfusion injury. When PEG-CAT was administered intrahepatically, GSH was significantly increased in the liver tissue following IRI (Figure 5C; P=0.002). When delivered systemically, the levels of GSH were not significantly different between livers that

received vehicle and those that received PEG-CAT following IRI, thus suggesting a lack of protection against IRI (Figure 5F).

To determine whether our non-significant results in Figure 5 D, E, and F were due to a lack of statistical power or were indeed non-significant, we conducted post hoc power analyses. With a sample number of 6 per group and an $\alpha = 05$ (two-tailed), our study had a 95% power (Cohen's d =2.08, large effect) to detect a difference in tissue MDA (Figure 5D), 80% power (Cohen's d =−1.61, large effect) to detect a difference in ATP (Figure 5E), and 99% power (Cohen's d =−2.49, large effect) to detect difference in total glutathione (Figure 5E). Overall, these analyses yield confidence that the non-significant effects found in the systemic administration data were not due to a lack of statistical power.

Direct Delivery of PEG-CAT to the Liver Maintains Hepatic Tissue Architecture

Centrilobular (acinar zone 3) necrosis is the hallmark of ischemic/hypoxic injury to the liver. A pathologist blinded to the groups examined the H&E sections of liver tissue after IRI. While some amount of vacuolation and minimal congestion was observed in both vehicle-treated and PEG-CAT treated groups, there was severe zone 2 and 3 hepatic necrosis with extra-sinusoidal red blood cells and microvascular thrombosis in the vehicle-treated group (Figure 6A). Hepatic architecture was relatively preserved in the PEG-CAT group compared to controls (Figure 6B). These findings were consistent with a statistically significant higher mean Suzuki score in the control (vehicle-treated) group compared to PEG-CAT group (Figure 6C; $P<0.0001$).

Direct Delivery of Alexa Fluor 488-labeled PEG-CAT to Liver Results in Improved Uptake by Liver Parenchyma

To further elucidate the pharmacokinetics of the PEG-CAT administered through this model, Alexa Fluor 488-labeled PEG-CAT was administered and evaluated histologically by fluorescence microscopy. When administered by direct intrahepatic injection via the portal vein, fluorescently labeled PEG-CAT remained in the liver parenchyma (Figure 6C). In contrast, when Alexa Fluor 488-labeled PEG-CAT was administered systemically via the femoral vein, fluorescently labeled PEG-CAT was not observed (Figure 6D).

Discussion

Hepatic injury secondary to ischemia/reperfusion remains an important consideration in the pathophysiology of acute disease states such as sepsis, trauma, and liver resection. This is especially true when hepatic injury occurs in the setting of underlying liver disease. IRI can lead to post-hepatectomy liver failure (PHLF) with incidence rates as high as 34% resulting in increased mortality and morbidity (30). Protective strategies against IRI such as ischemic preconditioning and pharmacological preconditioning have been previously investigated (31, 32). While the pharmacological preconditioning through exogenous administration of catalase previously demonstrated protection against IRI in various organs, success was limited by its short half-life, imprecise targeting, and large volume of distribution.

Pegylation (i.e., coupling catalase with polyethylene glycol) has been shown to increase the half-life of the enzyme by making the complex resistant to proteolytic degradation (19, 20,

33, 34). Pegylation does improve the therapeutic potential of catalase, but its predilection for the vascular endothelium makes systemic delivery of PEG-CAT challenging. Systemic delivery greatly increases the amount of the compound needed to protect the liver from IRI. While molecular targeting through mannosylation and galactosylation has been attempted with moderate success (17, 35), pegylation remains an attractive vehicle for the delivery of catalase to the liver due to its availability, ease of synthesis, and low toxicity.

Previous in vitro experiments have suggested that PEG-CAT preferentially targets the endothelium (20), which is a major site of oxidant injury. In our study, we show that PEG-CAT is taken up by all of the major cell types of the liver. This finding greatly increases the potential effectiveness of PEG-CAT to protect the liver during IRI. Furthermore, data indicate that hepatocytes and LSECs, in particular, were well-protected by PEG-CAT during oxidative stress injury. These cell types are important therapeutic targets to mitigate IRI, because they are particularly vulnerable during oxidative stress and play critical roles in the precipitation of pathophysiology associated with IRI. During oxidative stress, the electrochemical gradient across the mitochondrial membrane (or mitochondrial membrane potential) is critical for maintenance of oxidative phosphorylation and cellular respiration (36). Our in vitro data demonstrated that injury from oxidative stress disrupts the mitochondrial membrane potential resulting in cell death, while PEG-CAT pretreatment prolonged the stabilization of the mitochondrial membrane potential and enhanced cell viability.

Catalase is a natural antioxidant, and a critical component of the cellular antioxidant defense system. Therefore, direct administration of catalase does confer some protection against oxidative stress (17), but only partial protection against free radicals as seen during ischemic damage (18). To investigate whether the improved protection of PEG-CAT over non-pegylated catalase reported in the literature (20) might be due to more than just bioavailability, we compared the uptake and protective effects of non-pegylated catalase and pegylated catalase in vitro. We found that non-pegylated catalase was not taken up as efficiently as PEG-CAT (Supplemental Figure 1A,B). Additionally, we found that the cell viability of non-pegylated catalase-treated hepatocytes was similar to H_2O_2-only treated cells suggesting that non-pegylated catalase did not confer any significant protection against oxidative stress (Supplemental Figure 1C). This lack of protection could be due to the short half-life of catalase (~6 minutes), which is a significant limitation of the use of exogenous non-pegylated catalase as a therapeutic agent. These data suggest that the improved protection of PEG-CAT over non-pegylated catalase is likely due to enhanced bioavailability, which is consistent with the literature (20).

The bioavailability of systemically administered PEG-CAT has been one of the major limitations to its applicability. We showed that direct administration of PEG-CAT during ischemia of the liver results in a very high first-pass uptake, which allows for a more concentrated dose of PEG-CAT to be administered in a smaller volume of distribution. This uptake confers significant protection from IRI, which is demonstrated by attenuation in levels of ALT, AST, and MDA, and better tolerance to oxidative stress (GSH) and maintenance of cellular function (ATP). Although the systemic first-pass effect could be overcome by administration of larger doses of PEG-CAT, previous attempts to do so have

led to undesirable side-effects such as splenic hypertrophy and stimulation in mice and vacuolation in splenic macrophages in rats (33). Taken together, these data suggest that PEG-CAT reduces the harmful effects of oxidative stress in the liver and intrahepatic administration may overcome many of the known limitations of this potential therapy. Given this, PEG-CAT has therapeutic potential for many areas of liver surgery.

In general, short durations of ischemia are generally well-tolerated by patients with healthy livers. However, livers with underlying parenchymal diseases such as cirrhosis, non-alcoholic fatty liver disease (NALFD), and non-alcoholic steatohepatitis (NASH) tend to tolerate ischemia/reperfusion very poorly (37, 38), and would benefit tremendously from this type of liver-directed therapy Another area of potential therapeutic interest is in liver transplantation. The growing shortage of organs for liver transplantation (39), declining quality of organs (40), and increasing use of marginal organs (41, 42) has renewed interest in the mitigation of IRI. Enhanced protection of the organ would allow for the expansion of the donor pool and would decrease wait-list mortality. Normothermic ex-vivo liver perfusion (NEVLP) is a platform, currently in clinical trials, that would allow for the intrahepatic delivery of these therapeutic molecules directly to the donor organ. NEVLP allows for the separation of the ischemia and reperfusion events, thus allowing for time to augment the ROS defenses (e.g., antioxidants and ROS scavengers) with the delivery of exogenous antioxidants, prior to implantation. We have previously demonstrated that PEG-CAT delivered during NEVLP can confer protection against the injury that occurs during normothermia (43). Therapeutic interventions such as these may improve organ performance after transplantation and decrease graft loss.

While this novel approach to PEG-CAT administration offers promising results, our model did not include marginal (e.g., steatotic) livers. Future directions will involve the investigation of PEG-CAT in this setting, as well as an investigation of the protective effects of PEG-CAT in a model of hepatic resection and/or transplantation.

Conclusions

In summary, we showed that PEG-CAT is widely taken up by all liver cell types in vitro and is protective against oxidative stress. Targeted in vivo intrahepatic portal delivery of PEG-CAT results in a high first-pass hepatic uptake and confers significant protection from hepatic IRI compared to systemic delivery. The safety profile of PEG-CAT is well-established, and the ability to deliver a concentrated dose in a small volume of distribution enhances the effectiveness of this molecule. As such, intrahepatic portal delivery of PEG-CAT has great therapeutic potential in mitigating the effects of IRI in various disease states and during some operative procedures.

Supplementary Material

Refer to Web version on PubMed Central for supplementary material.

Acknowledgments

We would also like to acknowledge hepatic pathologist Dr. Martha Yearsley for her expertise in interpretation of histologic findings and Curtis Dumond for his technical assistance. All staining protocols were performed by the Ohio State University Solid Tumor Translational Science Laboratory.

Funding

This work was supported by NIH T32AI 106704-01A1 and the T. Flesch Fund for Organ Transplantation, Perfusion, Engineering, and Regeneration at The Ohio State University.

Abbreviations:

ALT	alanine aminotransferase
ATP	adenosine triphosphate
DMEM	Dulbecco's Modified Eagle Medium
FBS	fetal bovine serum
FITC	fluorescein isothiocyanate
GSH	glutathione
H_2O	water
H_2O_2	hydrogen peroxide
IACUC	Institutional Animal Care and Use Committee
IRI	Ischemia-reperfusion injury
LSECs	Liver sinusoidal endothelial cells
MDA	malondialdehyde
O_2	oxygen
PEG-CAT	polyethylene glycol-catalase
ROS	Reactive oxygen species
SOD	superoxide dismutase
TBA	thiobarbituric acid
NALFD	non-alcoholic fatty liver disease
NASH	non-alcoholic steatohepatitis.

References

1. Smyrniotis V, Theodoraki K, Arkadopoulos N, Fragulidis G, Condi-Pafiti A, et al. Ischemic preconditioning versus intermittent vascular occlusion in liver resections performed under selective vascular exclusion: a prospective randomized study. The American Journal of Surgery 2006:192:669–674. [PubMed: 17071204]

2. Clavien PA, Yadav S, Sindram D, Bentley RC Protective Effects of Ischemic Preconditioning for Liver Resection Performed Under Inflow Occlusion in Humans. Ann Surg2000:155–162. [PubMed: 10903590]

3. Patel A, van de Poll MCG, Greve JWM, Buurman WA, Fearon KCH, et al. Early Stress Protein Gene Expression in a Human Model of Ischemic Preconditioning. Transplantation 2004:78.

4. Vollmar B, Glasz J, Post S, Menger MD Role of Microcirculatory Derangements in Manifestation of Portal Triad Cross-Clamping-Induced Hepatic Reperfusion Injury. Journal of Surgical Research 1996:60:49–54. [PubMed: 8592431]

5. Schindl MJ, Redhead DN, Fearon KCH, Garden OJ, Wigmore SJ The value of residual liver volume as a predictor of hepatic dysfunction and infection after major liver resection. Gut 2005:54:289. [PubMed: 15647196]

6. Vauthey J-N, Pawlik TM, Ribero D, Wu T-T, Zorzi D, et al. Chemotherapy Regimen Predicts Steatohepatitis and an Increase in 90-Day Mortality After Surgery for Hepatic Colorectal Metastases. Journal of Clinical Oncology 2006:24:2065–2072. [PubMed: 16648507]

7. Poon Ronnie TP, Fan ST Hepatectomy for hepatocellular carcinoma: Patient selection and postoperative outcome. Liver Transplantation 2004:10:S39–S45.

8. Ali Jason M, Davies Susan E, Brais Rebecca J, Randle Lucy V, Klinck John R, et al. Analysis of ischemia/reperfusion injury in time - zero biopsies predicts liver allograft outcomes. Liver Transplantation 2014:21:487–499.

9. Serracino-Inglott F, Habib NA, Mathie RT Hepatic ischemia-reperfusion injury. Am J Surg 2001:181:160–166. [PubMed: 11425059]

10. Vollmar B, Glasz J, Leiderer R, Post S, Menger MD Hepatic microcirculatory perfusion failure is a determinant of liver dysfunction in warm ischemia-reperfusion. Am J Pathol 1994:145:1421–1431. [PubMed: 7992845]

11. Saidi RF, Kenari SKH Liver Ischemia/Reperfusion Injury: an Overview. Journal of Investigative Surgery 2014:27:366–379. [PubMed: 25058854]

12. Weigand K, Brost S, Steinebrunner N, Büchler M, Schemmer P, et al. Ischemia/Reperfusion Injury in Liver Surgery and Transplantation: Pathophysiology. HPB Surg 2012:2012.

13. Fondevila C, Busuttil RW, Kupiec-Weglinski JW Hepatic ischemia/reperfusion injury--a fresh look. Exp Mol Pathol 2003:74:86–93. [PubMed: 12710939]

14. Held P An Introduction to Reactive Oxygen Species Measurement of ROS in Cells. Vinooski, Vermont: BioTek Instruments, Inc., 2012:1–14.

15. Chen CF, Hsueh CW, Tang TS, Wang D, Shen CY, et al. Reperfusion Liver Injury—Induced Superoxide Dismutase and Catalase Expressions and the Protective Effects of N-Acetyl Cysteine. Transplantation Proceedings 2007:39:858–860. [PubMed: 17524832]

16. Fujita T, Furitsu H, Nishikawa M, Takakura Y, Sezaki H, et al. Therapeutic effects of superoxide dismutase derivatives modified with mono- or polysaccharides on hepatic injury induced by ischemia/reperfusion. Biochemical and Biophysical Research Communications 1992:189:191–196. [PubMed: 1449473]

17. Yabe Y, Nishikawa M, Tamada A, Takakura Y, Hashida M Targeted delivery and improved therapeutic potential of catalase by chemical modification: combination with superoxide dismutase derivatives. J Pharmacol Exp Ther 1999:289:1176–1184. [PubMed: 10215702]

18. Atalla SL, Toledo-Pereyra LH, Mackenzie GH, Cederna JP INFLUENCE OF OXYGEN-DERIVED FREE RADICAL SCAVENGERS ON ISCHEMIC LIVERS. Transplantation 1985:40:584–589. [PubMed: 2866612]

19. Pyatek P, Abuchowski A, Davis F Preparation of a polyethylene glycol: superoxide dismutase adduct, and an examination of its blood circulation life and anti-inflammatory activity. Des Commun Chem Pathol Pharmacol. 1980:29:113–127.

20. Beckman JS, Minor RL, White CW, Repine JE, Rosen GM, et al. Superoxide dismutase and catalase conjugated to polyethylene glycol increases endothelial enzyme activity and oxidant resistance. J Biol Chem 1988:263:6884–6892. [PubMed: 3129432]

21. Beal EW, Dumond C, Kim J-L, Mumtaz K, DH Jr., et al. Method of Direct Segmental Intra-hepatic Delivery Using a Rat Liver Hilar Clamp Model. Journal of Visual Experiments (JOVE) 2017:122.

22. Bale SS, Geerts S, Jindal R, Yarmush ML Isolation and co-culture of rat parenchymal and non-parenchymal liver cells to evaluate cellular interactions and response. Scientific Reports 2016:6:25329. [PubMed: 27142224]
23. Leask A, Chen S, Pala D, Brigstock DR Regulation of CCN2 mRNA expression and promoter activity in activated hepatic stellate cells. J Cell Commun Signal. Dordrecht: 2008:49–56.
24. Zeng W A New Method to Isolate and Culture Rat Kupffer Cells. 2013.
25. Nishikawa M, Hashida M, Takakura Y Catalase delivery for inhibiting ROS-mediated tissue injury and tumor metastasis. Advanced Drug Delivery Reviews 2009:61:319–326. [PubMed: 19385054]
26. Suzuki S, Nakamura S, Koizumi T, Sakaguchi S, Baba S, et al. The beneficial effect of a prostaglandin I2 analog on ischemic rat liver. Transplantation 1991:52:979–983. [PubMed: 1750084]
27. Mahmoudian J, Hadavi R, Jeddi-Tehrani M, Mahmoudi AR, Bayat AA, et al. Comparison of the Photobleaching and Photostability Traits of Alexa Fluor 568- and Fluorescein Isothiocyanate-conjugated Antibody. Cell J 2011:13:169–172. [PubMed: 23508937]
28. Panchuk-Voloshina N, Haugland RP, Bishop-Stewart J, Bhalgat MK, Millard PJ, et al. Alexa Dyes, a Series of New Fluorescent Dyes that Yield Exceptionally Bright, Photostable Conjugates. Journal of Histochemistry & Cytochemistry 1999:47:1179–1188. [PubMed: 10449539]
29. Scandalios JG Oxidative stress responses - what have genome-scale studies taught us?, Genome Biol. London: 2002:reviews1019.1011–1016.
30. Rahnemai-Azar AA, Cloyd JM, Weber SM, Dillhoff M, Schmidt C, et al. Update on Liver Failure Following Hepatic Resection: Strategies for Prediction and Avoidance of Post-operative Liver Insufficiency. J Clin Transl Hepatol2018:97–104. [PubMed: 29577036]
31. Turrens JF, Crapo JD, Freeman BA Protection against oxygen toxicity by intravenous injection of liposome-entrapped catalase and superoxide dismutase. J Clin Invest 1984:73:87–95. [PubMed: 6690485]
32. Yabe Y, Kobayashi N, Nishihashi T, Takahashi R, Nishikawa M, et al. Prevention of neutrophil-mediated hepatic ischemia/reperfusion injury by superoxide dismutase and catalase derivatives. Journal of Pharmacology and Experimental Therapeutics 2001:298:894–899. [PubMed: 11504782]
33. Viau AT, Abuchowski A, Greenspan S, Davis FF Safety evaluation of free radical scavengers PEG-catalase and PEG-superoxide dismutase. J Free Radic Biol Med 1986:2:283–288. [PubMed: 3584850]
34. Muzykantov VR Targeting of superoxide dismutase and catalase to vascular endothelium. J Control Release 2001:71:1–21. [PubMed: 11245904]
35. Yabe Y, Kobayashi N, Nishikawa M, Mihara K, Yamashita F, et al. Pharmacokinetics and Preventive Effects of Targeted Catalase Derivatives on Hydrogen Peroxide-Induced Injury in Perfused Rat Liver. Pharmaceutical Research 2002:19:1815–1821. [PubMed: 12523659]
36. Hüttemann M, Lee I, Pecinova A, Pecina P, Przyklenk K, et al. Regulation of oxidative phosphorylation, the mitochondrial membrane potential, and their role in human disease. Journal of Bioenergetics and Biomembranes 2008:40:445. [PubMed: 18843528]
37. op den Dries S, Sutton ME, Lisman T, Porte RJ Protection of Bile Ducts in Liver Transplantation: Looking Beyond Ischemia. Transplantation 2011:92.
38. Merion RM, Goodrich NP, Feng S How can we define expanded criteria for liver donors? Journal of Hepatology 2006:45:484–488. [PubMed: 16905221]
39. UNOS Transplant trends | UNOS. 2017.
40. Orman ES, Mayorga ME, Wheeler SB, Townsley RM, Toro-Diaz HH, et al. Declining liver graft quality threatens the future of liver transplantation in the United States. Liver Transpl 2015:21:1040–1050. [PubMed: 25939487]
41. Attia M, Silva MA, Mirza DF The marginal liver donor – an update. Transplant International 2008:21:713–724. [PubMed: 18492121]
42. Busuttil The utility of marginal donors in liver transplantation. Liver transplantation 2003:9:651–663. [PubMed: 12827549]
43. Beal EW, Dumond C, Kim J-L, Akateh C, Eren E, et al. A Small Animal Model of Ex Vivo Normothermic Liver Perfusion. JoVE 2018:e57541.

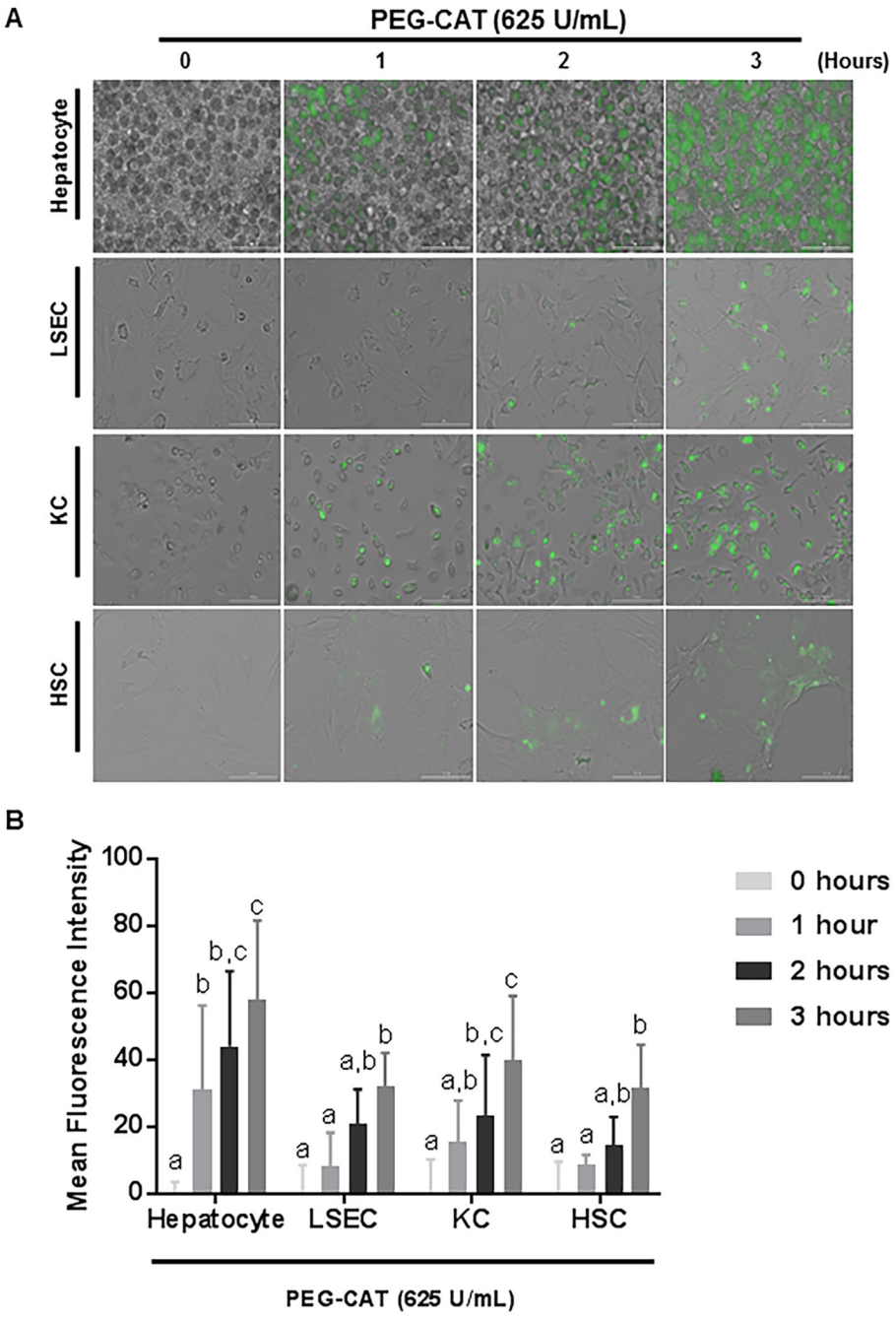

Figure 1: FITC-labeled PEG-CAT is taken up by hepatocytes, liver sinusoidal endothelial cells (LSECs), Kupffer cells (KCs), and hepatic stellate cells (HSCs).

FITC-labeled PEG-CAT was taken up by all liver cells indicating that localized/directed treatment may be a preferred method. **(A)** Micrographs at 0, 1, 2, and 3 hours post-treatment with FITC-labeled PEG-CAT show increased uptake by all cell types in a time-dependent manner with hepatocytes taking up the most in the least amount of time. **(B)** Quantification of FITC-labeled PEG-CAT uptake is shown by the mean fluorescence intensity plotted at each time interval. The bar graphs show the mean fluorescence intensity of FITC-labeled

PEG-CAT ± SD from three independent cell cultures. Values in bar graphs not sharing a letter indicate a significant difference at $P<0.05$.

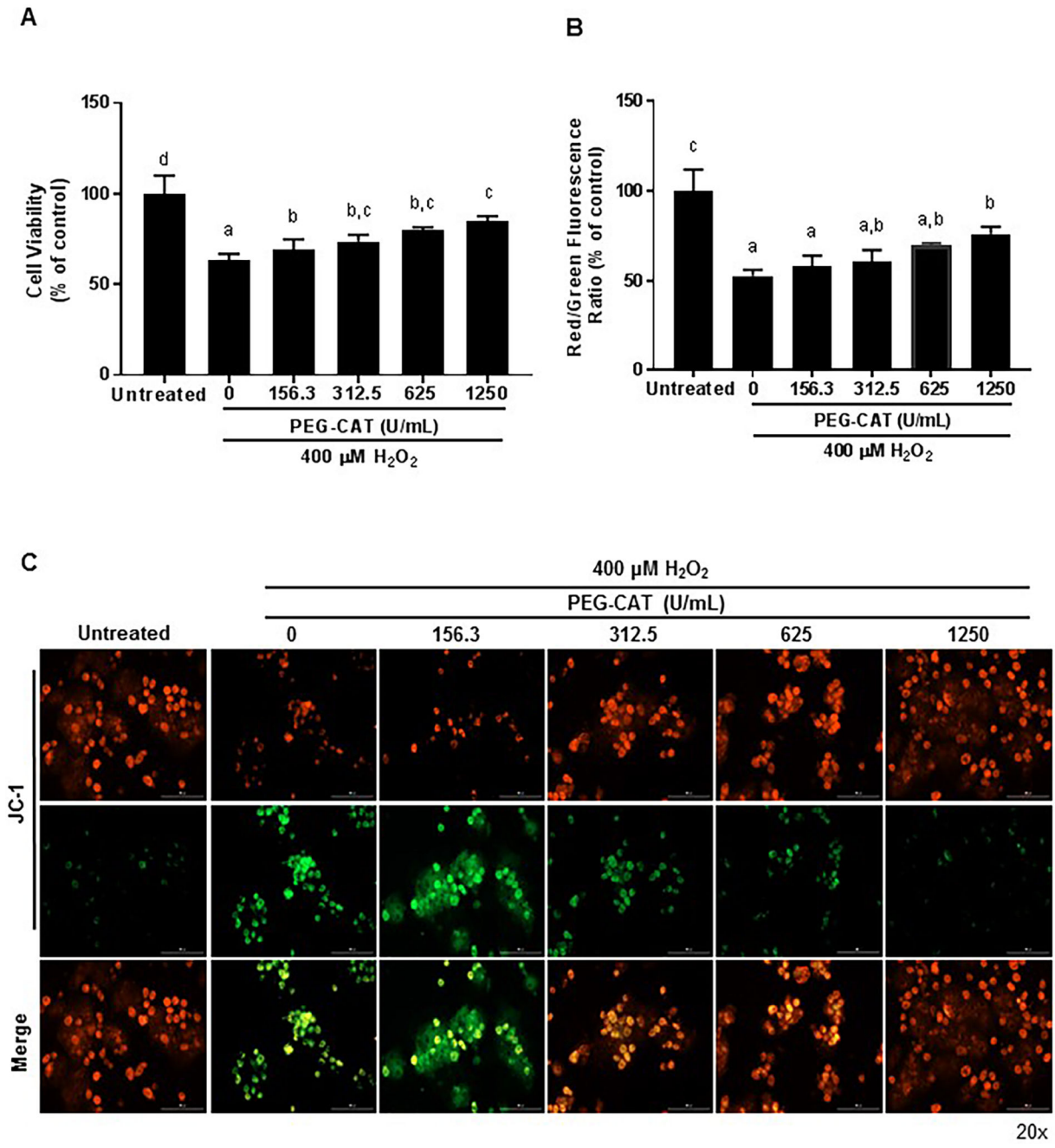

Figure 2: PEG-CAT protects hepatocytes from oxidative injury in a dose-dependent manner.

Hepatocytes were plated for 24 hours and treated with varying doses of PEG-CAT for 3 hours. Cells were then washed and treated with 400 μM H_2O_2 for 3 hours to induce oxidative stress. **(A)** Post-oxidative stress injury, PEG-CAT increased cell viability in a dose-dependent manner. Bar graphs show the mean absorbance relative to control ± SD from each of three independent cell cultures. Values in bar graphs not sharing a letter indicate a significant difference at $P<0.05$. **(B)** Mitochondrial membrane potential (MMP) was determined in hepatocytes by fluorescent JC-1 staining where the ratio of JC-1 red/green fluorescence represents the MMP. Data were obtained from three independent cell culture

experiments. Bar graphs represent the mean ratio of JC-1 red/green fluorescence relative to the untreated control group ± SD. Values in bar graphs not sharing a letter indicate a significant difference at $P<0.05$. **(C)** Representative fluorescence micrographs of hepatocytes after JC-1 staining illustrate a dose-dependent increase in mitochondrial protection during oxidative stress. Red puncta represent JC-1 polymers/aggregates (normal membrane potential), while green puncta represent JC-1 monomers (depolarized MMP/damaged mitochondria).

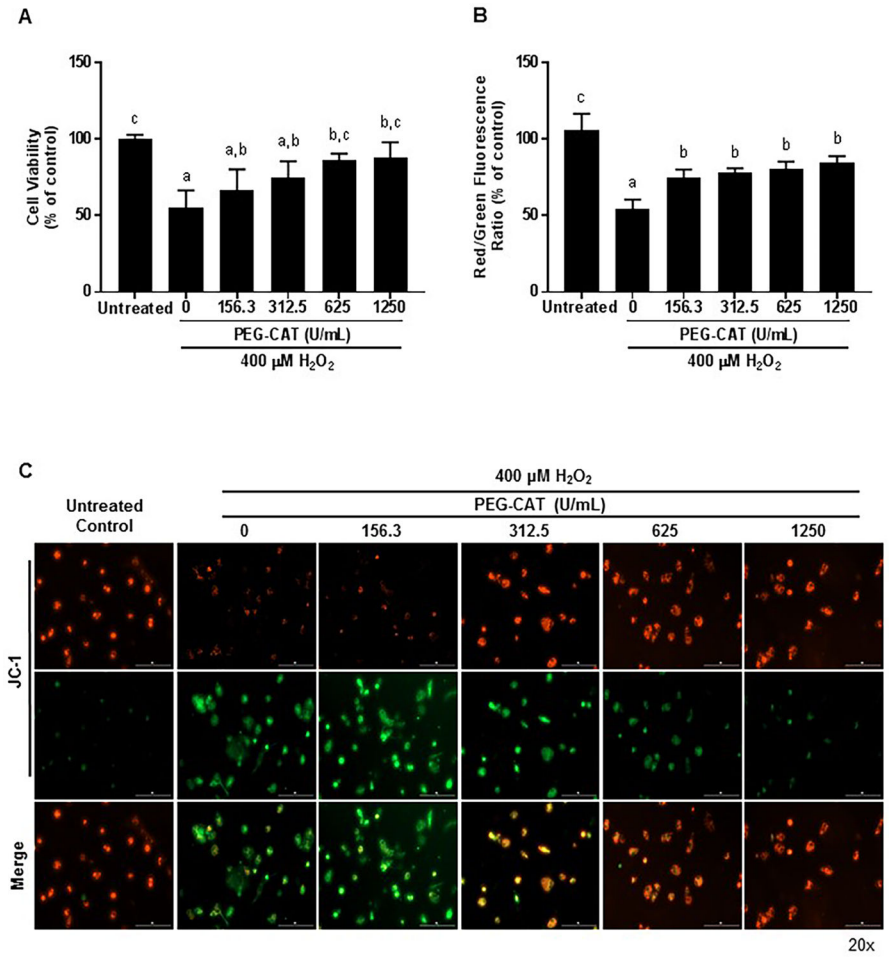

Figure 3: PEG-CAT protects liver sinusoidal endothelial cells (LSECs) from oxidative injury in a dose-dependent manner.

LSECs were plated for 24 hours and treated with varying doses of PEG-CAT for 3 hours. Cells were then washed and treated with 400 μM H_2O_2 for 3 hours to induce oxidative stress. **(A)** PEG-CAT increased cell viability of LSECs in a dose-dependent manner post-oxidative injury. Bar graphs show the mean absorbance relative to control ± SD from each of three independent cell cultures. Values in bar graphs not sharing a letter indicate a significant difference at $P<0.05$. **(B)** Mitochondrial membrane potential (MMP) was determined in LSECs by fluorescent JC-1 staining where the ratio of JC-1 red/green fluorescence represents the MMP. Data were obtained from three independent cell cultures. Bar graphs represent the mean ratio of JC-1 red/green fluorescence relative to the untreated control group ± SD. Values in bar graphs not sharing a letter indicate a significant difference at $P<0.05$. **(C)** Representative fluorescence micrographs of LSECs after JC-1 staining illustrate a dose-dependent increase in mitochondrial protection during oxidative stress. Red puncta represent JC-1 polymers/aggregates (normal membrane potential), while green puncta represent JC-1 monomers (depolarized MMP/damaged mitochondria).

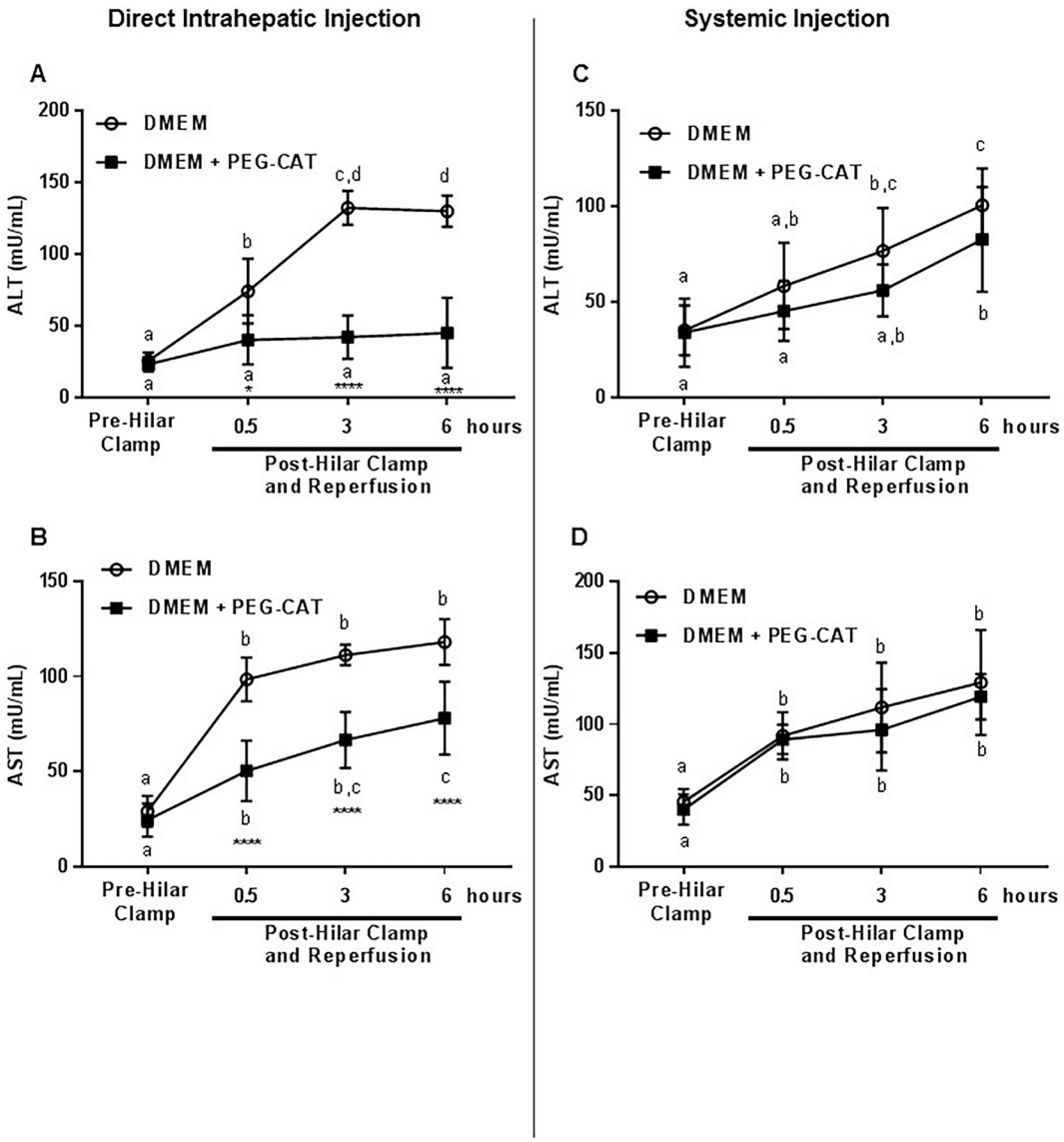

Figure 4: Direct delivery of PEG-CAT into liver attenuates hepatic injury.

PEG-CAT or DMEM was injected into the left portal vein (direct intrahepatic) and IRI was then induced in the liver. In a second group, PEG-CAT or DMEM was injected into the left femoral vein (systemic) and IRI was then induced in the liver. After 1 hour, the livers were reperfused and serum was obtained at 0.5, 3, and 6 hours of reperfusion. **(A)** AST and **(B)** ALT levels in serum were significantly decreased with intrahepatic PEG-CAT. Systemic delivery of PEG-CAT did not result in a significant change in serum **(C)** ALT and **(D)** AST compared to controls. Mean ± SD (n=6 per group) values are plotted against time of collection. Values in bar graphs not sharing a letter indicate a significant difference between time points within a group at $P<0.05$. Asterisks signify statistically significant differences between treatment groups at each time point. (** $P<0.01$, **** $P<0.0001$).

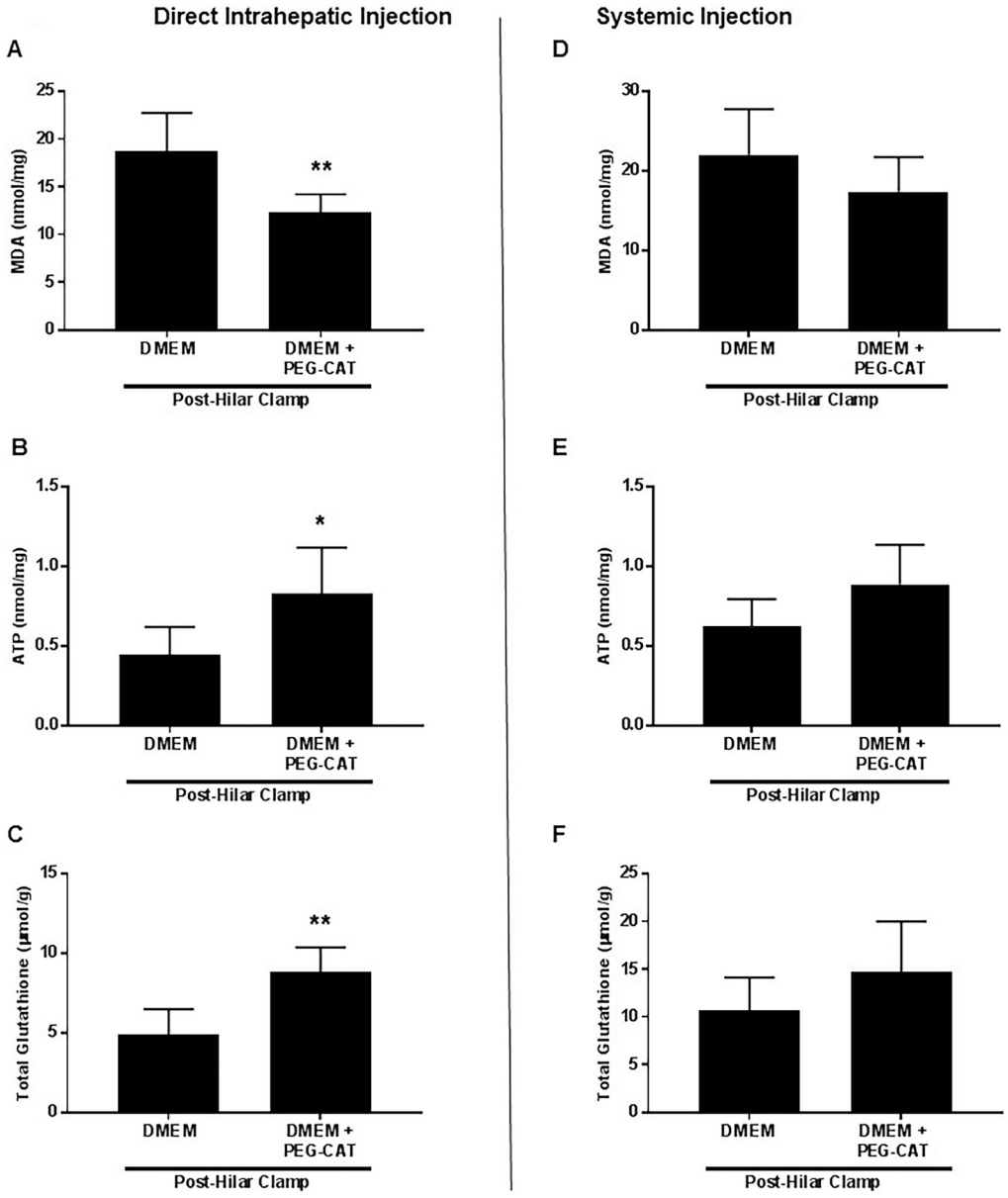

Figure 5: Direct delivery of PEG-CAT into the liver leads to decreased MDA and increased ATP and GSH in liver tissue, while systemic delivery fails to offer the same protection from hepatic injury.

Ischemia was induced in the liver after injection of PEG-CAT into the left portal vein (direct intrahepatic). In a second experimental group, ischemia was induced in the liver after delivery of PEG-CAT into the left femoral vein (systemic). After 1 hour of ischemia, the liver was reperfused for 6 hours and liver tissue was procured. **(A)** Tissue MDA was significantly decreased in the intrahepatic PEG-CAT delivery group compared to vehicle control, while **(D)** no significant difference was seen in the systemic delivery group. Intrahepatic PEG-CAT delivery resulted in increased **(B)** ATP and **(C)** GSH tissue levels compared to vehicle control. Systemic PEG-CAT delivery resulted in no differences in **(E)** ATP or **(F)** GSH levels compared to vehicle control. The data displayed are from 6

independent experiments. Asterisks signify statistically significant differences (* $P<0.05$, ** $P<0.01$).

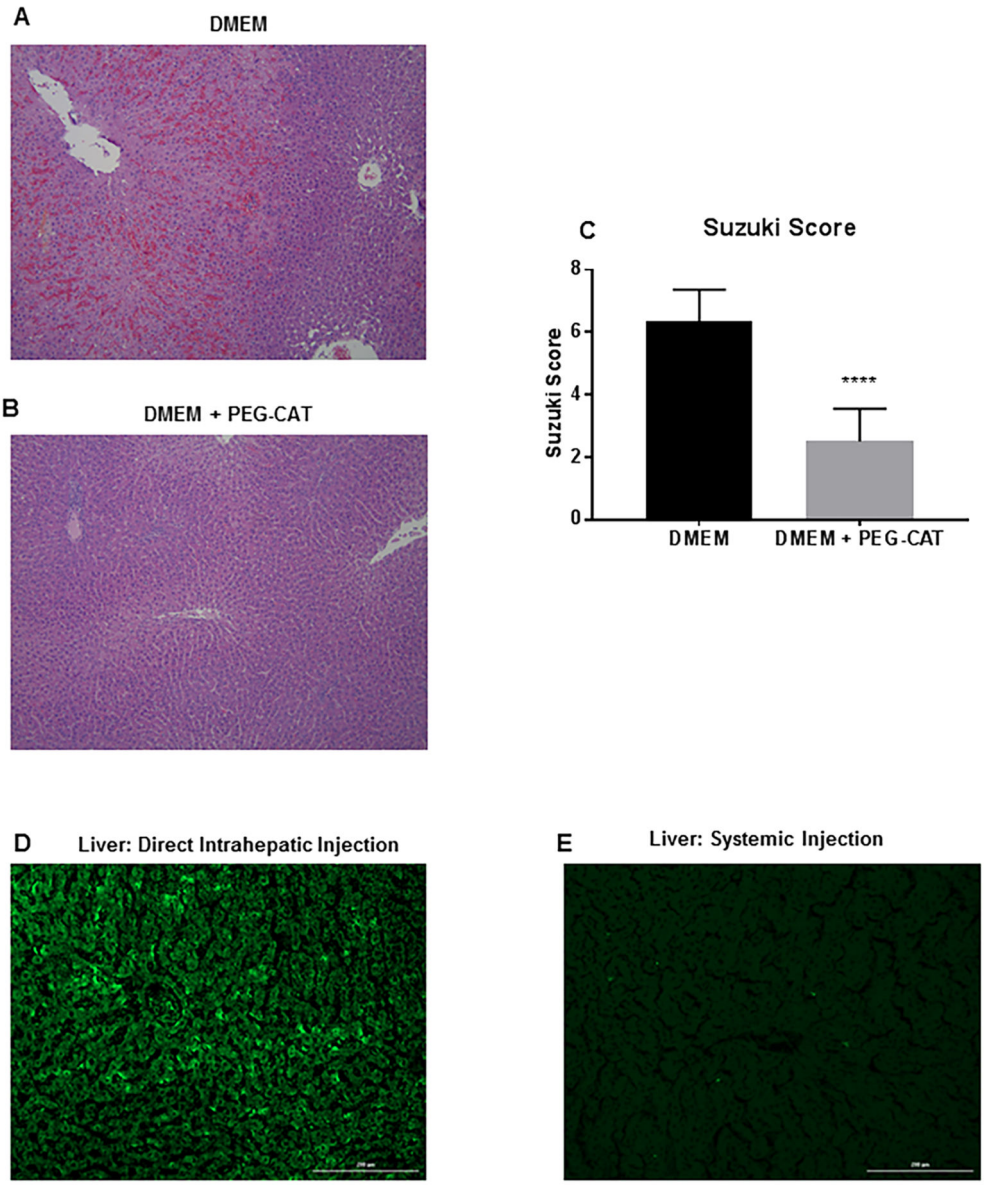

FIGURE 6: Direct intrahepatic administration of PEG-CAT maintains hepatic architecture during ischemia/reperfusion.

Alexa Fluor 488-labeled PEG-CAT or DMEM was injected into the left portal vein, and then ischemia was induced in the liver. After 1 hour of ischemia and 6 hours of reperfusion, the liver was processed for H&E staining. **(A)** A representative colorimetric micrograph from six independent experiments demonstrates zone 2 and 3 hepatocyte necrosis, extrasinusoidal red blood cells, and thrombosis in DMEM-treated livers **(B)** and that the liver parenchyma was better protected by intrahepatic PEG-CAT administration. The degree of liver injury is quantified via the Suzuki score. (**C**) A lower score, corresponding to lower levels of congestion, vacuolization, and necrosis, was seen in the PEG-CAT group compared to DMEM-treated livers. Fluorescence micrographs of the liver were taken from rats injected with Alexa-Fluor 488-labeled PEG-CAT either directly into the liver **(D)** or systemically through the femoral vein **(E)**. When Alexa-Fluor 488-labeled PEG-CAT injected into the left

portal vein (intrahepatic delivery), Alexa Fluor 488-labeled PEG-CAT was taken up into the hepatic parenchyma, but minimal uptake occurred when injected systemically. Asterisks signify statistically significant differences (**** $P<0.0001$).